Journal of Molecular Catalysis A: Chemical 398 (2015) 203–214

Contents lists available at ScienceDirect

Journal of Molecular Catalysis A: Chemical

journal homepage: www.elsevier.com/locate/molcata

Influence of the support on the selective ring opening of methylcyclohexane and decalin catalyzed by Rh–Pd catalysts

Silvana A. D'Ippolito[a], Catherine Especel[b], Laurence Vivier[b], Stéphane Pronier[b], Florence Epron[b], Carlos L. Pieck[a,*]

[a] Instituto de Investigaciones en Catálisis y Petroquímica (INCAPE) (FIQ-UNL, CONICET), Santiago del Estero 2654, 3000 Santa Fe, Argentina
[b] Université de Poitiers, CNRS UMR 7285, Institut de Chimie des Milieux et Matériaux de Poitiers (IC2MP), 4 rue Michel Brunet, TSA 51106, 86073 Poitiers Cedex 9, France

ARTICLE INFO

Article history:
Received 14 September 2014
Received in revised form 4 December 2014
Accepted 5 December 2014
Available online 16 December 2014

Keywords:
Rh–Pd
Bifunctional catalysts
Ring opening
Decalin
Methylcyclohexane

ABSTRACT

Rh–Pd catalysts supported on Al_2O_3, SiO_2 and SiO_2–Al_2O_3 (SIRAL 40) were studied for methylcyclohexane (MCH) and decalin ring opening reactions. It was found that the Rh/Pd atomic ratios were similar to the theoretically expected one and the metal dispersion values varied between 30 and 50%. On bimetallic catalysts supported on Al_2O_3 and SiO_2, Pd and Rh were present mainly in the form of monometallic particles, whereas a heterogeneous distribution constituted of large Pd particles and small bimetallic ones were observed on SIRAL 40. Total and Bronsted acidities followed the order: SIRAL 40 » Al_2O_3 > SiO_2. Al_2O_3 supported catalysts were the most suitable for MCH ring opening, while the opening of decalin was favored by using SiO_2–Al_2O_3 (SIRAL 40). The catalysts supported on SiO_2 produced mainly dehydrogenated compounds. The higher total and Bronsted acidities of SIRAL 40 series had a great impact on the opening of bicyclic naphthenes, whereas the metal function of the catalyst and the hydrogenolytic activity of Rh had a major role during MCH reaction. Using bimetallic catalysts in the MCH reaction decreased the formation of cracking and dehydrogenated products, and the selective formation of RO products could be optimized by tuning the working temperature.

1. Introduction

LCO (Light cycle oil) is a waste stream from the bottom of the fluid catalytic cracking (FCC) unit that is used for heating and is added to heavy fuel to adjust its viscosity [1]. Due to the increasing diesel demand, an interesting application would be to combine the LCO fraction to the diesel pool. However, the LCO characteristics are very different from the diesel fuel specifications Therefore, the LCO fraction must be subjected to major changes. The content of sulfur and nitrogen can be reduced by conventional hydrotreating [2] and the polycyclic aromatic by hydrogenation to improve the cetane index (CI). However, this improvement is not sufficient and it is necessary to open the naphthenic rings [3,4]. The CI increases considerably when decalin is converted to linear or monobranched paraffins. The selective ring opening (SRO) of naphthenes is a very complex chemistry, largely depending on the operating conditions and characteristics of the catalyst system [5].

The support has a strong influence on the SRO reaction because the interaction with the metallic particles can change their electronic properties and the presence of acid sites can significantly change the chemistry of the process [6]. The zeolites with larger pore size, such as HY, are considered as among the most suitable supports for this purpose. In general, the use of zeolites of large pore size favors the ring opening reaction, limiting the deactivation due to coke deposits [7–9]. Also the size of the crystal [10], the number and distribution of the strength of Bronsted acid sites [10,11] are important parameters for obtaining ring opening (RO) products. Santana et al. reported in a study devoted to ring opening of decalin and tetralin that Pt/HY is more effective than HY without metallic promoters [12]. Pt in Pt/USY bifunctional catalysts significantly increases the rate of isomerization and thus the formation of ring opening products compared to monofunctional USY catalysts. It has been shown that the addition of Pt to acidic materials reduces the strength of Bronsted acid sites and significantly improves the isomerization and ring opening of decalin [13]. The use of zeolites can lead to non-selective cracking (undesirable side reactions) and pore constraints issue steric impediments [7,12,14,15].

The opening reaction of C_6 naphthenes is enhanced by the use of bifunctional catalysts [16–19]. This can be explained considering that on the acid function of the catalyst takes place contraction of C_6 ring to C_5 one, which is easier to open on the metal function [4,18,19]. Kustov et al. [20] studied Pt, Rh, Ru and Ni catalysts

* Corresponding author. Tel.: +54 342 4533858; fax: +54 342 4531068.
E-mail address: pieck@fiq.unl.edu.a (C.L. Pieck).

http://dx.doi.org/10.1016/j.molcata.2014.12.011
1381-1169/

supported on alumina and silica for ring opening (RO) of cyclohexane in conditions close to the industrial ones. It was observed that Rh catalysts have higher activity and inhibit the dehydrogenation reaction as compared to the Pt catalysts. Other authors [13,21] also proposed and studied Rh-based catalysts for the reaction of SRO due to their large hydrogenolytic capacity. Metals such as Pt, Pd, Ir, Ru and Rh supported on Al_2O_3 were observed as active and selective for RO of methylcyclopentane to C_6 paraffins [22,23].

It was reported that the hydrogenolytic activity follows the order: Pt < Rh < Ir < Ru [24,25]. Over bifunctional catalysts, characterized by the presence of acidic sites and a hydro-dehydrogenating function, the reactions occur via carbenium ions, i.e., β-scission and isomerization. Do et al. [5] pointed out that decalin ring opening is catalyzed both by the acid function through β-scission and by the metal via dicarbene mechanism leading to highly isomerized products.

The research has begun with noble metal catalysts supported on mesoporous silica-based materials [7,26]. In this type of bifunctional catalysts the acid function allows the contraction of the ring, and then the metal sites more easily produce hydrogenolysis of C—C bonds. The silica–alumina mixed phases contain not only silica–alumina, but also pure silica and aluminum groups which exhibit strong Bronsted acid sites with strengths comparable to that of zeolites [27]. The concentration of Bronsted acid sites can be adjusted by varying the silica content [28]. This support is presented as an alternative to zeolites that commonly lead to excessive cracking activity.

In previous works [29,30], we studied the influence of the SiO_2/Al_2O_3 ratio and the Rh–Pd content on the ring opening of methylcyclohexane and decalin using silica–alumina as support. In line with this research, this work studies the influence of the support (Al_2O_3, SiO_2 and Al_2O_3–SiO_2) on the properties of Rh and Pd monometallic and Rh–Pd bimetallic catalysts. The objective is to optimize the metal/acid functions for favoring the selective opening of the rings of methylcyclohexane and decalin.

2. Experimental

2.1. Catalysts preparation

γ-Al_2O_3 (Cyanamid Ketjen CK-300, pore volume = 0.5 $cm^3\,g^{-1}$, Sg = 180 $m^2\,g^{-1}$), SiO_2 (SIL, pore volume = 0.31 $cm^3\,g^{-1}$, Sg = 130 $m^2\,g^{-1}$) and SiO_2–Al_2O_3 provided by Sasol (SIRAL 40, 60.7 and 39.3 wt% of Al_2O_3 and SiO_2, respectively; pore volume = 0.9 $cm^3\,g^{-1}$, Sg = 514 $m^2\,g^{-1}$) were used as support. Previously, they were calcined at 450 °C for 4 h (10 °C min^{-1}, air, 60 $cm^3\,min^{-1}$). Rh and Pd were added by a common coimpregnation method. An aqueous solution of HCl (0.2 mol L^{-1}) was added to the support and the system was left unstirred at room temperature for 1 h. Then an aqueous solution of $RhCl_3$ and/or $PdCl_2$ (Sigma–Aldrich) was added in order to have a total metal charge of 1 wt%. For the bimetallic catalysts, the Rh/Pd atomic ratio was 0.5, 1 and 2. The slurry was gently stirred for 1 h at room temperature and then it was put in a thermostated bath at 70 °C until a dry solid was obtained. Drying was completed in a stove at 120 °C overnight. Finally, the samples were calcined in flowing air (60 $cm^3\,min^{-1}$) at 300 °C for 4 h and reduced under flowing H_2 (60 $cm^3\,min^{-1}$, 500 °C, 4 h). The monometallic catalysts were named Pd1 or Rh1/support while the bimetallic catalysts were named Rx/support, Rx corresponding to the Rh/Pd atomic ratio.

2.2. Measurement of the Pd and Rh contents

The composition of the metal function was determined by inductively coupled plasma-optical emission spectroscopy (ICP–OES) after digestion of the sample in an acid solution and dilution. Chlorine contents of catalysts in their final state, i.e., after activation, were measured with the Charpentier–Volhard method, in which the sample was dissolved in concentrated sulfuric acid and Cl ions precipitated with silver nitrate solution. Excess silver solution was back titrated with a thiocyanate solution to give the amount of chlorine on the original sample.

2.3. Temperature programmed desorption of pyridine

This test was used for measuring the amount and strength of the acid sites. Samples of 200 mg were impregnated with an excess of pyridine. The samples were then rinsed and the excess of physisorbed pyridine was eliminated by heating the sample in a nitrogen stream at 110 °C for 1 h. Then the temperature was raised at a rate of 10 °C min^{-1} to a final value of 700 °C. To measure the amount of desorbed pyridine, the reactor exhaust was connected to a flame ionization detector. The error associated to the peak position and areas has been determined to be of about 7% [31].

2.4. Isomerization of 3,3-dimethyl-1-butene (33DM1B)

The equipment used was described previously [29]. The catalyst (50 mg) was pretreated in situ, by reduction with H_2 (60 $cm^3\,min^{-1}$, 450 °C, 1 h). The sample was then cooled in N_2 (30 $cm^3\,min^{-1}$) to the reaction temperature adjusted in order to have small conversion values to avoid secondary reactions. Then the feed from the saturator was injected. The reagent partial pressure and flow rate were 20.9 kPa and 15.2 mmol h^{-1}, respectively. The error associated to the test of 33DM1B isomerization was determined by calculating the variance of the conversion in a set of seven experiments (variance = 6.5%).

2.5. H_2 chemisorption

This technique was used in order to estimate the metallic accessibility of the Pd, Rh and Rh–Pd particles on the surface of the catalyst. The sample (100 mg) was reduced at 500 °C (10 °C min^{-1}, H_2 30 $cm^3\,min^{-1}$) for 1 h. Then argon (30 $cm^3\,min^{-1}$) was made to flow over the sample for 2 h at 500 °C in order to eliminate adsorbed hydrogen. Finally the sample was cooled down to 70 °C in argon and calibrated pulses of H_2 were injected into the reactor (HC1). These pulses were sent until the sample was saturated. After flushing the system with argon during 30 min, a second set of pulses was injected (HC2). The difference HC1–HC2 allows one to estimate the metallic accessibility considering the stoichiometry between a hydrogen atom and a Pd or Rh surface atom (H/Pd and H/Rh) equal to 1.

2.6. Transmission electron microscopy (TEM) measurements

TEM measurements were performed on a JEOL 2100 electron microscope operating at 200 kV with a LaB_6 source and equipped with a Gatan ultra scan camera. The powder was ultrasonically dispersed in ethanol, and the suspension was deposited on an aluminum grid coated with a porous carbon film. Average particle sizes were determined by measuring at least 100 particles for each sample analyzed, from at least five different micrographs. The particle size distribution was obtained from TEM pictures calculating the surface average particle diameter from $d = \Sigma n_i d_i^3 / \Sigma n_i d_i^2$. Microanalysis of Pd and Rh was carried out by energy dispersive X-ray spectroscopy (EDX) in the nanoprobe mode.

2.7. Temperature programmed reduction (TPR)

The tests were performed in an Ohkura TP2002 apparatus equipped with a thermal conductivity detector. At the beginning of each TPR test, the catalyst samples were pretreated in situ by heating in air at 400 °C for 1 h. Then they were heated from 0 to 700 °C at 10 °C min^{-1} in a gas stream of 5.0% hydrogen in argon (molar base).

2.8. Fourier transform infrared (FTIR) spectroscopy study of adsorbed CO

Transmission FTIR spectra were collected in the single-beam mode, with a resolution of 2 cm^{-1}, using a Nicolet Nexus FTIR spectrometer. Catalyst samples were prepared as self-supported wafers with a diameter of 12 mm and a "thickness" of approximately 20 mg cm^{-2}. Prior to CO adsorption experiments, all the catalysts were reduced in situ for 1 h under H_2 at 500 °C, then outgassed at this temperature before to be cooled to room temperature. Reference spectra of the clean surfaces were collected at room temperature. CO was introduced to the cell by small doses up to saturation, and was then purged to remove any weakly bonded CO. Spectra were collected until a steady state was reached. Difference spectra between the samples and the corresponding reference are shown in this paper.

2.9. Cyclopentane hydrogenolysis

The equipment used was described previously [29]. Before the reaction, the catalysts were reduced for 1 h at 500 °C in hydrogen (60 cm^3 min^{-1}). Then they were cooled down in hydrogen to the reaction temperature (300 °C). The other conditions were: catalyst mass = 150 mg, pressure = 0.1 MPa, H_2 flow rate = 36 cm^3 min^{-1}, cyclopentane (CP) flow rate = 0.483 cm^3 h^{-1}. The error in the conversion value in the CP hydrogenolysis test is about 8%.

2.10. Cyclohexane dehydrogenation

The equipment used was described previously [29]. Reaction conditions were: catalyst mass = 50 mg, temperature = 350 °C, pressure = 0.1 MPa, H_2 flow rate = 36 cm^3 min^{-1}, cyclohexane (CH) flow rate = 1.61 cm^3 h^{-1}. Before the reaction the catalysts were reduced in hydrogen (60 cm^3 min^{-1}, 500 °C, 1 h). The average error of the measurements was less than 3% [31].

2.11. Ring opening of methylcyclohexane (MCH)

MCH hydrogenolysis was performed in gas phase in a fixed-bed continuous reactor described previously [29]. Reaction conditions were: catalyst mass = 1.5 g, total pressure = 3.9 MPa, molar ratio H_2/MCH = 8, WHSV = 2 h^{-1} and temperature = 250–450 °C. Previously, the catalysts were reduced in situ at the reaction pressure at 500 °C for 1 h using 60 cm^3 min^{-1} of H_2. The conversion was varied by changing the reaction temperature, in 25 °C steps. The initial reaction temperature was chosen according to the metal loading and the support of each catalyst. After reaching a conversion near 100%, the temperature was not increased more. Four measurements were performed at each temperature; the values given in the results correspond to the average of these four measurements. The absence of intra and extra granular diffusion limitations in these experimental conditions were checked [29]. The error associated with the data was at maximum 5%.

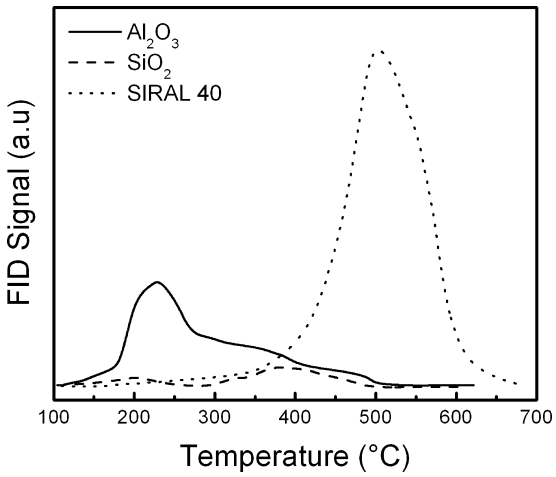

Fig. 1. Temperature programmed desorption of pyridine of the supports.

2.12. Ring opening of decalin

The reaction conditions were: stainless steel autoclave reactor, temperature = 350 °C, hydrogen pressure = 3 MPa, stirring rate = 1360 rpm, volume of decalin = 25 cm^3, catalyst loading = 1 g. The decalin had 37.5% *cis* isomer and a *trans*/*cis* ratio of 1.63. The experiments conditions and the equipment were described previously, also it was checked that diffusional limitations to mass transfer are negligible [30].

3. Results and discussion

3.1. Metal content

Table 1 shows the Rh/Pd atomic ratio as well as the weight percentage of Rh and Pd as determined by ICP analysis and the theoretical values for all prepared mono and bimetallic catalysts. The R1/SIRAL 40 presents the highest difference between the deposited and theoretical total metal content (25%). This difference is lower for the SiO_2 supported catalysts. However, whatever the catalyst, the difference between the deposited and theoretical Rh/Pd atomic ratio is at most of 6%.

3.2. Evaluation of the acidity by TPD of pyridine and isomerization of 33DM1B

Fig. 1 shows the profiles of pyridine temperature programmed desorption (TPD) determined on the three supports. The SIRAL 40 support presents a peak at 503 °C, and the alumina a peak with a maximum at 225 °C and a shoulder extending from 270 to 500 °C. Finally the silica shows two small peaks at 202 and 387 °C. The desorption temperature is associated with the strength of the acid sites and the area under the TPD curve indicates the total acidity. SIRAL 40 presents a high concentration of strong acid sites; Al_2O_3 has weak to moderate acidity, as SiO_2, but in larger quantities. As indicated at the bottom of Table 2, the total acidity, referred to SiO_2, is equal to 5.2 and 14.8 for Al_2O_3 and SIRAL 40, respectively. The addition of Pd and Rh increases the total acidity on the three supports (Table 2). This could be due to the presence of Cl^- incorporated by the metal precursors or by the HCl used as competitor to produce a homogeneous metal distribution on the support [32]. In a previous work, we found that Al_2O_3–Cl has about three times more acidity than Al_2O_3 [33]. As it can be seen in Table 2, the chlorine content is in correlation with the total acidity. The electronic interaction of the metal particles with the support could be responsible for the changes in acidity. Some authors reported the same behav-

Table 1
Percentage (wt%) of Rh and Pd and Rh/Pd atomic ratio determined by ICP analysis.

Catalyst	Rh[a] (wt%)	Rh[b] (wt%)	Pd[a] (wt%)	Pd[b] (wt%)	Pd + Rh[b] (wt%)	Rh/Pd[b]
$Pd1/Al_2O_3$	–	–	1.00	0.83	0.83	–
$R0.5/Al_2O_3$	0.33	0.31	0.67	0.61	0.92	0.53
$R1/Al_2O_3$	0.49	0.43	0.51	0.43	0.86	1.03
$R2/Al_2O_3$	0.66	0.56	0.34	0.28	0.84	2.07
$Rh1/Al_2O_3$	1.00	0.81	–	–	0.81	–
$Pd1/SiO_2$	–	–	1.00	0.87	0.87	–
$R0.5/SiO_2$	0.33	0.29	0.67	0.59	0.88	0.51
$R1/SiO_2$	0.49	0.47	0.51	0.46	0.93	1.06
$R2/SiO_2$	0.66	0.55	0.34	0.29	0.84	1.96
$Rh1/SiO_2$	1.00	0.91	–	–	0.91	–
Pd1/SIRAL40	–	–	1.00	0.78	0.78	–
R0.5/SIRAL40	0.33	0.26	0.67	0.54	0.80	0.5
R1/SIRAL40	0.49	0.36	0.51	0.39	0.75	0.95
R2/SIRAL40	0.66	0.52	0.34	0.28	0.80	1.92
Rh1/SIRAL40	1.00	0.79	–	–	0.79	–

[a] Theoretical.
[b] Determined by ICP.

ior pointing to the importance of the redistribution of the acid sites [13,34–41].

The conversion values for the isomerization reaction of 33DM1B were taken as a measure of the concentration of Brønsted acid sites. Kemball and co-workers [42,43] demonstrated that the Lewis acid sites are not involved in this reaction. Only two isomers are formed (2,3-dimethyl-2-butene and 2,3-dimethyl-1-butene) at low reaction temperature (<300 °C) [44]. The SiO_2 series was not evaluated in 33DM1B isomerization due to the low acidity of the support. The activities of Al_2O_3 and SIRAL 40 for the 33DM1B isomerization were evaluated as a function of temperature between 100 and 300 °C. The activation energy is of 63.5 and 35.6 kJ mol^{-1} on Al_2O_3 and SIRAL 40, respectively, indicating that SIRAL 40 is by far the support presenting the highest concentration of Bronsted acid sites. Consequently, for comparing the effect of the presence of the metal on both supports, the reaction was performed at 100 °C for the SIRAL 40 series and at 250 °C for the Al_2O_3 one. Fig. 2 shows the conversion extrapolated at zero reaction time for the monometallic and R1 bimetallic catalysts supported on Al_2O_3 and for the complete SIRAL 40 series. It must be noticed that the differences between the catalysts of each series are very difficult to infer because the experimental error is 6.5%. It is important to point out that the Bronsted acidity depends strongly on the support and is affected to a lesser degree

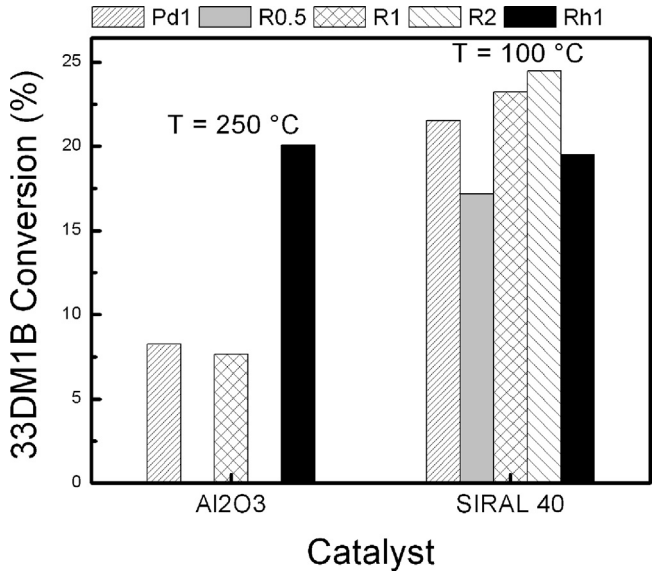

Fig. 2. Initial conversion values for the 33DM1B isomerization of the catalysts supported on Al_2O_3 and SIRAL 40.

Table 2
Pyridine TPD area (relative to SiO_2), chlorine content (wt%), chemisorption values (H/M) and metal particle sizes (d).

Catalyst	Pyridine	Chlorine	H/M (%)	d[b] (nm)
	TPD[a]	(wt%)		
$Pd1/Al_2O_3$	13.5	0.9	16	5.4
$R0.5/Al_2O_3$	18.6	0.88	39	2.3
$R1/Al_2O_3$	16.4	0.92	42	2.1
$R2/Al_2O_3$	14.1	0.94	45	1.9
$Rh1/Al_2O_3$	13.1	0.89	43	1.9
$Pd1/SiO_2$	4.9	0.7	32	2.9
$R0.5/SiO_2$	4.9	0.69	33	2.7
$R1/SiO_2$	4.7	0.72	31	2.9
$R2/SiO_2$	4.3	0.73	33	2.6
$Rh1/SiO_2$	4.9	0.68	30	2.8
Pd1/SIRAL40	40.5	1.4	37	2.5
R0.5/SIRAL40	48.1	1.41	50	1.8
R1/SIRAL40	50.2	1.44	46	1.9
R2/SIRAL40	56.9	1.39	34	2.6
Rh1/SIRAL40	44.4	1.37	36	2.3

[a] Pyridine TPD area relative to SiO_2:SiO_2 = 1.00, Al_2O_3 = 5.2; SIRAL 40 = 14.8.
[b] Deduced from H_2 chemisorption.

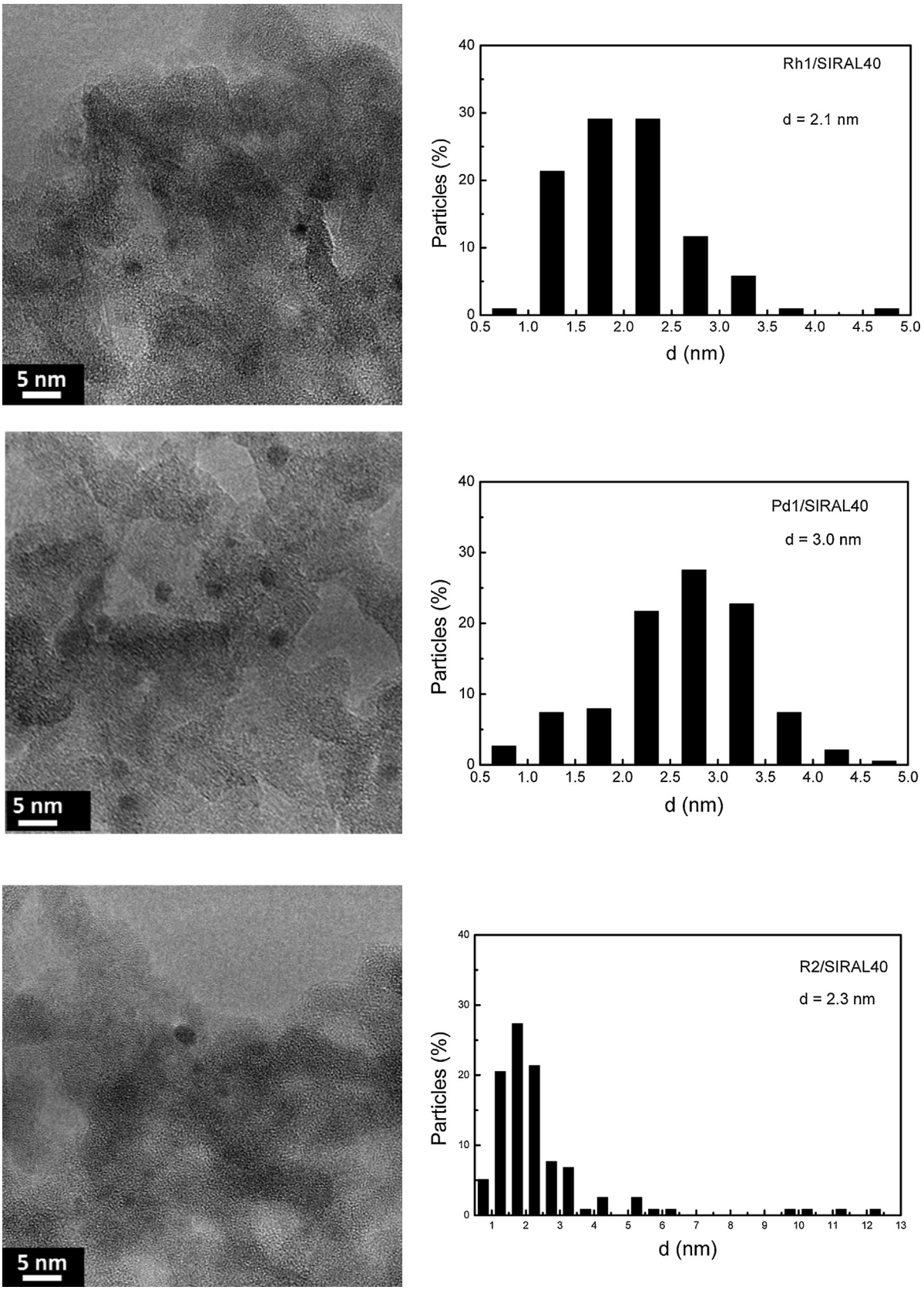

Fig. 3. Representative TEM images and particle size distribution for SIRAL 40 supported catalysts.

by the nature of the metal, especially on the most acidic support (SIRAL 40).

3.3. Hydrogen chemisorption and TEM analysis

Table 2 shows the hydrogen chemisorptions values ($H/(Rh+Pd)$ in %) of the catalysts. Monometallic catalysts, i.e., Pd1 and Rh1 samples, exhibit quite comparable H/M values for a given support, except in the case of $Rh1/Al_2O_3$ which displays a greater dispersion than $Pd1/Al_2O_3$ (43% compared to 16%). In the case of the bimetallic catalysts supported on SIRAL 40, the metal dispersion decreases when increasing the Rh content. An opposite behavior is found for the Al_2O_3 series while SiO_2 supported catalysts show no appreciable changes. The monometallic Rh or bimetallic catalysts supported on SiO_2 present lower dispersion than their counterparts supported on SIRAL 40 and Al_2O_3. This may be due to the absence of anion exchange capacity of the SiO_2 support, leading therefore to less metal-support interaction and favoring thus the migration of species and the development of large crystals.

For the sake of simplicity, only TEM pictures of catalysts supported on SIRAL 40 are presented (Fig. 3). In agreement with the values of hydrogen chemisorption TEM experiments show that metal particles are well dispersed on the Al_2O_3 and SIRAL 40, except on $Pd1/Al_2O_3$. The particles have a mean diameter between 2.1 and 3.0 nm, not very different from the mean diameters determined from H_2 chemisorption results (Table 2). The R2/SIRAL40 sample shows some large particles around 10 nm, which were analyzed by EDX as corresponding to monometallic Pd particles. On this sample, bimetallic particles were also identified with a majority of particles enriched in Rh, with Rh/Pd atomic ratio between 2.66 and 3.30. Similar results were reported by Hensen et al. [28] who found the formation of very small well-dispersed PdRh alloy particles and few bigger particles which might correspond to some isolated single metal aggregates (Pd preferentially located on the particle surfaces). On the $R2/Al_2O_3$ sample, most of the particles are monometallic, with small Pd particles about 1 nm and larger Rh particles of 2 nm, also some bimetallic particles with Rh/Pd atomic ratio around 1.6 were analyzed, i.e., with more Pd than the nominal value. In conclusion, TEM and EDX analysis show that is more difficult to obtain an homogeneous particle size distribution on SIRAL 40 than on Al_2O_3.

3.4. TPR

The degree of metal-metal and metal-support interactions were evaluated by temperature programmed reduction (TPR). Fig. 4 shows the TPR profiles of the three series of catalysts. In all cases, the hydrogen consumption indicates that the metals are completely reduced at temperatures below 500 °C. Monometallic Pd and Rh catalysts supported on Al_2O_3 show a reduction peak with a maximum at 75 °C and 143 °C, respectively. When supported on alumina, Pd is reduced at a lower temperature compared to the other supports. It was shown by TEM that Pd particles supported on alumina are mostly agglomerated with a mean size of 5.8 nm determined from H_2 chemisorption. Then, it can be inferred that the presence of Pd agglomerates, with low metal-support interactions favor the reduction of Pd oxides. On the Pd-containing catalysts, whatever the support, no reduction peak was observed at room temperature which would be assigned to a reduction of large Pd-oxide species, according to the lirerature [45].

Bimetallic catalysts supported on Al_2O_3 have a single reduction peak between 122 and 133 °C, suggesting a simultaneous reduction of Pd and Rh oxides. The increase in Rh content shifts the reduction of the metal phase to higher temperatures. On the bimetallic $R2/Al_2O_3$ catalyst, TEM demonstrated that Pd is either as monometallic well dispersed nanoparticles with diameter around 1 nm or in bimetallic particles. Then, compared to the $Pd1/Al_2O_3$ catalyst, the shift of the reduction peak to higher temperatures may be attributed to both the reduction of smaller Pd monometallic particles in strong interaction with the support and the co-reduction of Pd and Rh.

Pd1 and Rh1 catalysts supported on SiO_2 show a reduction peak at 100 and 132 °C, respectively, and bimetallic catalysts exhibit a similar behavior to those supported on Al_2O_3.

In the case of monometallic catalysts supported on SIRAL 40, the reduction ends at temperatures higher than 250 °C, which can be ascribed to the presence of very small metal particles in strong interaction with the support. In addition, for the R0.5 and R1 bimetallic catalysts, the peaks clearly appear to be composed of

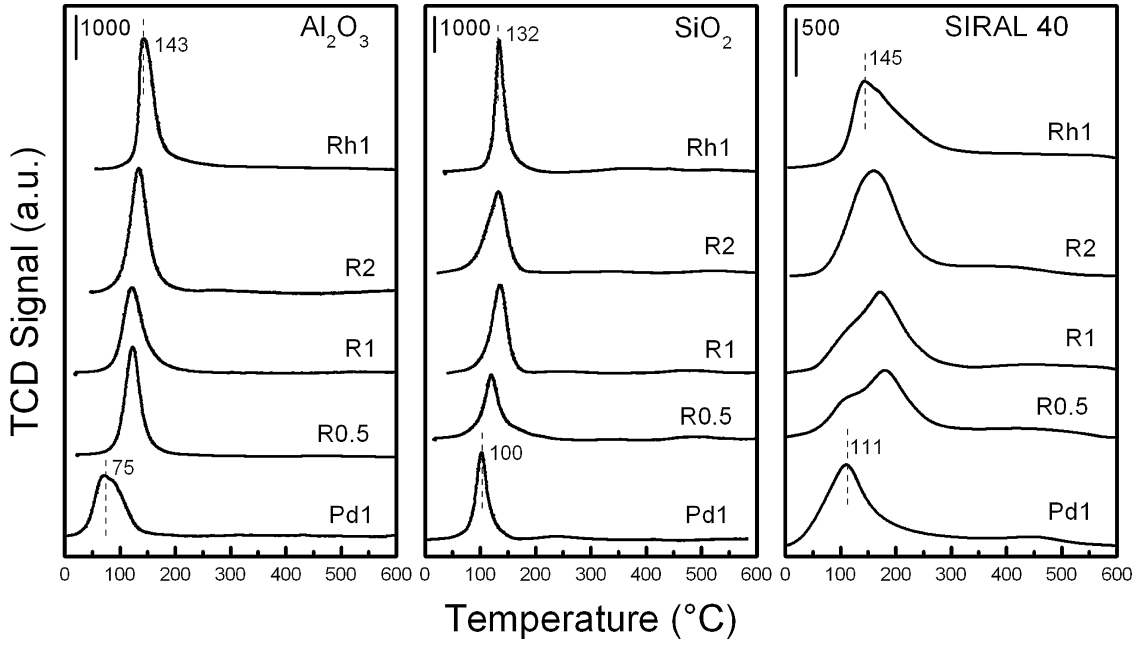

Fig. 4. Temperature programmed reduction of the catalysts.

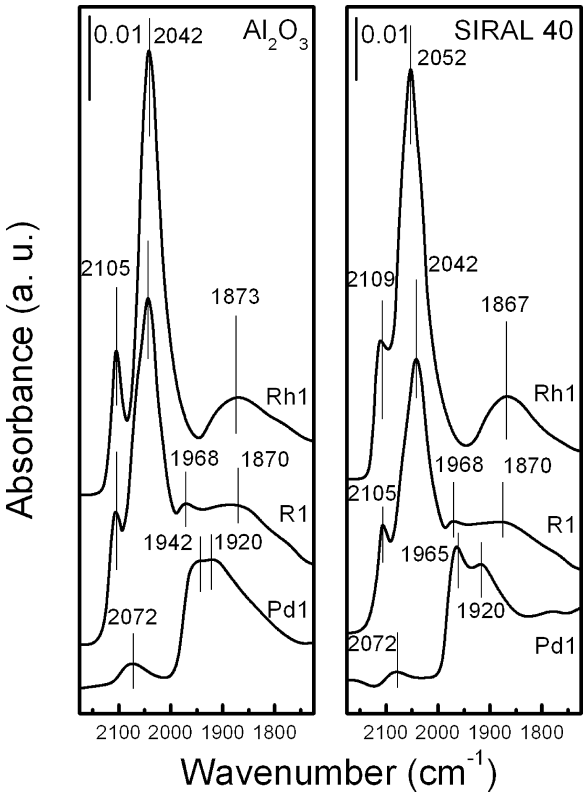

Fig. 5. CO–FTIR spectrum of the Pd1 and Rh1 monometallic catalysts and R1 bimetallic catalysts supported on Al_2O_3 and SIRAL 40.

at minimum 2 peaks, one around 110 °C, attributable to the reduction of monometallic palladium particles, and another one at 175 °C due to the reduction of oxides Rh particles. In agreement with the TEM and EDX analysis, it seems that it is more difficult to obtain a homogeneous particle size distribution on the SIRAL 40 support than on Al_2O_3.

It is important to point out that the TPR trace of the monometallic Rh catalysts supported on Al_2O_3 and SiO_2 show only one reduction peak. This implies that all the rhodium species immobilized on the respective support material possess the same redox properties. Meanwhile, the broad reduction peak and the shoulder found in the Rh1/SIRAL40 catalyst indicate the presence of rhodium species with different redox properties.

3.5. CO–FTIR results

The CO–FTIR spectra of the monometallic and R1 bimetallic catalysts supported on Al_2O_3 and SIRAL 40 are show in Fig. 5. Metallic palladium forms carbonyls that are generally characterized by bands at wavenumbers below 2100 cm^{-1} [46–48], with, in general, one band around 2100 cm^{-1} attributed to linearly bonded CO (L band), and broad and convoluted bands below 1995 cm^{-1} assigned to bridged CO (B band). The band corresponding to bridged CO species may be decomposed into three main types of species: B1, close to 1970 cm^{-1}, and B2, around 1955 cm^{-1}, corresponding to di-coordinated bridged CO species on two types of Pd planes and a band below 1830 cm^{-1} generally assigned to triply bonded CO species [49]. The spectra of CO adsorbed on Pd1/SIRAL40 and Pd1/Al_2O_3 present peaks attributable to linear and doubly bridged CO.

The monometallic catalysts of Rh1/Al2O3 and Rh1/SIRAL 40 show three bands centered at 2107 ± 2 cm^{-1}, 2047 ± 5 cm^{-1} and 1870 ± 3 cm^{-1}. According to Yang and Garland [50], the broad bands in the 1800–1900 cm^{-1} range may be ascribed to bridged CO species

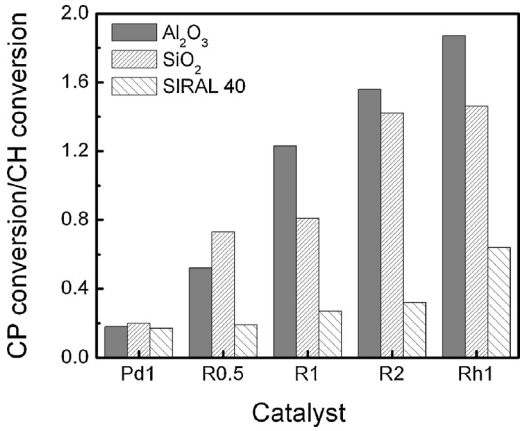

Fig. 6. Cyclopentane conversion/cyclohexane conversion ratio obtained in the cyclopentane hydrogenolysis and cyclohexane dehydrogenation.

adsorbed on Rh^0. The two other bands may be attributed to gem-dicarbonyl $Rh^+(CO)_2$ species in agreement with Smith et al. [51], who demonstrated that the vibrational frequencies of $Rh^+(CO)_2$ supported on alumina appears in the region 2105–2088 cm^{-1} for the symmetric and 2040–2016 cm^{-1} for the antisymmetric vibrations. Consequently, the bands at 2107 ± 2 cm^{-1} and 2047 ± 5 cm^{-1} observed on the Rh1 catalysts are attributed to the vibrations of the gem-dicarbonyl $Rh^+(CO)_2$ species with symmetric and antisymmetric modes, respectively, [52–54]. The presence of Rh^+ species is generally explained by Rh oxidation in presence of CO involving hydroxyl groups of the support [55].

R1/Al2O3 and R1/SIRAL 40 bimetallic catalysts show similar FTIR–CO absorption bands with a preponderance of the bands corresponding to CO adsorbed on rhodium at 2105, 2042 and 1870 cm^{-1}. Both bimetallic catalysts have a band at 1968 cm^{-1}, which may be attributed to bridged CO species adsorbed on Pd. Due to the complexity of the spectra obtained on mono and bimetallic catalysts, it is not possible to clearly conclude on particular interactions between Pd and Rh in the bimetallic catalysts from the CO–FTIR spectra.

3.6. Dehydrogenation of cyclohexane and hydrogenolysis of cyclopentane

The reaction of cyclohexane (CH) dehydrogenation to benzene can be used as an indirect method to characterize the metal sites on supports of mild to moderate acidity such as alumina or silica; the reaction rate is proportional to the active surface metal atoms. It is considered insensible to the structure of the catalyst, i.e., it does not need a special ensemble of atoms [56]. Inversely, cyclopentane (CP) hydrogenolysis is a structure–sensitive reaction, which requires a number of metal atoms with a given configuration [22]. CP conversion/CH conversion ratio (noted CP/CH) represents the ratio between a demanding reaction and a non-demanding one. It can be seen in Fig. 6 that the CP/CH ratio increases with the Rh content in the three catalyst series, which means that, with the increase in Rh loading, the hydrogenolytic behavior dominates over the dehydrogenating ones. This is an important data because during naphthenic ring opening reaction the dehydrogenation to aromatics must be decreased while hydrogenolysis must be favored.

3.7. MCH ring opening

Fig. 7 shows the conversion values of MCH as a function of the reaction temperature for the three series supported on Al_2O_3, SiO_2 and SIRAL 40. As expected, for all the catalysts the conversion increases with the reaction temperature. It was reported that crack-

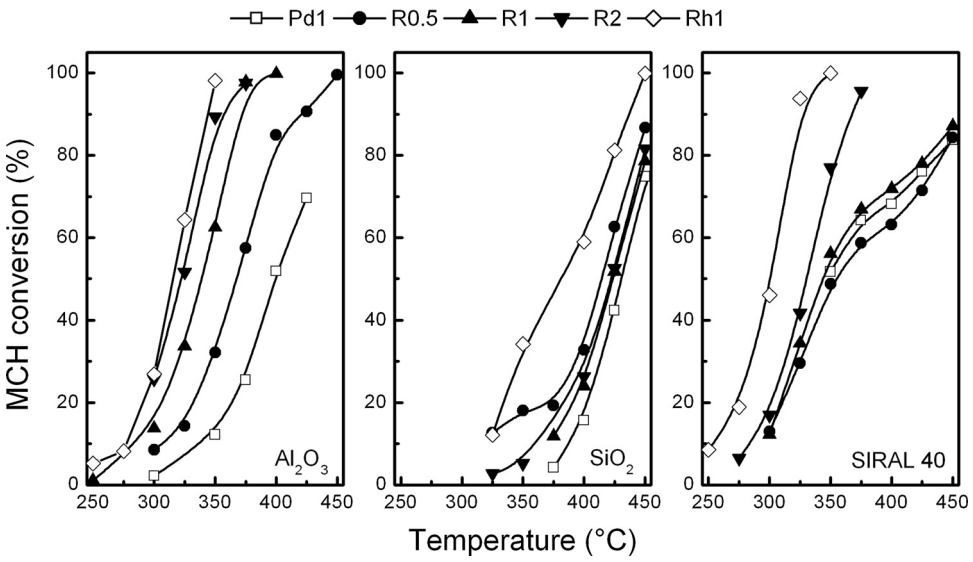

Fig. 7. MCH conversion as a function of the temperature reaction for the three series of catalysts.

ing of MCH is an irreversible endothermic reaction that is favored at high temperature [10,57,58]. Previous experiments have shown that the deactivation occurring during the MCH reaction was negligible. This was checked by the following procedure. After having reached the highest reaction temperature and the maximum conversion, the temperature was decreased by steps of 25 °C to the lowest one. The MCH conversions as well as the products distribution obtained were similar.

Monometallic catalysts supported on SIRAL 40 show higher conversion values at a given temperature than the ones of the Al_2O_3 and SiO_2 series. In the three series, the Rh1 catalysts display a higher activity than the Pd1 ones, in agreement with the higher hydrogenolytic activity of Rh, as previously demonstrated. Bimetallic catalysts have an intermediate activity between those of the Rh1 and Pd1 catalysts, except for the R0.5/SIRAL40 catalyst which exhibits an activity slightly lower than the Pd1/SIRAL40 sample. On the SiO_2 supported catalysts, higher temperatures are needed to reach the conversion range of the other supported catalysts. The lower activity of the SiO_2 supported samples is probably due to their low acidity as reported in Table 2.

The reaction products of MCH are classified in: (i) cracking products, i.e., C_1–C_6 resulting from either deep hydrogenolysis or acidic cracking; (ii) isomerization products, i.e., saturated cyclic alkanes containing the same number of carbon atoms as MCH but with C_5 ring; (iii) ring opening (RO) products, i.e., C_7 alkanes resulting from the opening of MCH and its isomers; and (iv) dehydrogenation products, i.e., toluene.

The selectivities were calculated by dividing the yield to each kind of products by the amount of MCH converted, as previously reported [59]. Fig. 8 shows the selectivity to ring opening products as function of the conversion for each catalyst series. The ring opening selectivity decreases with increasing MCH conversion due to deep hydrogenolysis and cracking [17]. For each series, Rh1 catalyst is more selective to RO than the corresponding Pd1 one. The bimetallic catalysts show the following order of selectivity to RO products, according to the nature of the support: Al_2O_3 > SIRAL 40 > SiO_2. At low conversions, the selectivity to RO increases with the Rh content on Al_2O_3 and SIRAL 40 series, probably due to the increase of the hydrogenolysis activity, as previously highlighted by the CP/CH ratio. The bimetallic catalysts supported on SiO_2 show an opposite trend, with slight variations as function of the metal composition. At high conversions (close to 80%), the R0.5/Al_2O_3, R0.5/SiO_2 and R2/SIRAL40 catalysts exhibit finally the highest selectivity to RO among all bimetallic catalysts of each series. Fig. 9 shows the selectivity to cracking, isomerization, ring opening and dehydrogenation products as a function of the conversion obtained with these three catalysts. It can be seen that the selectivities to isomerization and ring opening decrease as the conversion increases, due to cracking of these products on R0.5/Al_2O_3 and R2/S40 and due to dehydrogenation on R0.5/SiO_2. Finally, the R2/SIRAL40 and R0.5/Al_2O_3 catalysts display a good combination of metal and acid functions, allowing the preferential ring opening of MCH by a bifunctional mechanism, involving a contraction step of the C_6 ring to alkylcyclopentanes with a subsequent opening to paraffins. It is obvious that the selectivity is affected by the support acidity and by the composition of the metallic phase. Catalysts with low total and Bronsted acidity, such those supported on SiO_2, produce mainly dehydrogenated compounds and low amounts of isomers and cracking products. On the other hand, catalysts with high total and Bronsted acidity, such those supported on SIRAL 40, produce more cracking products and higher amounts of isomers. R0.5/Al_2O_3 catalyst has selectivity to dehydrogenated products higher than that of R2/SIRAL40 due to its higher content Pd, which favors more dehydrogenation than hydrogenolysis. However, by considering the metal function only, the CP/CH ratio was previously observed to be higher on R0.5/Al_2O_3 catalyst than on R2/SIRAL40 (Fig. 6).Then, less dehydrogenated products would be expected on R0.5/Al_2O_3 because hydrogenolysis reaction might prevail on the metallic sites. The negligible formation of dehydrogenated products on R2/SIRAL40 catalyst could be due to the high acidity that favors the MCH ring contraction and the subsequent ring opening of the as-formed C_5 ring.

Among the cracking products, the major part is constituted of C_1 and C_6 products, mainly produced by hydrogenolysis on the metallic function. It can be seen in Fig. 10 that the C_1 and C_6 products increase linearly with the yield to cracking products for the three series of catalysts. An acid-catalyzed cracking would have yield C_3 and C_4 products.

From the MCH reaction, it can be concluded that, on all supports, it is possible to reduce both the formation of cracking and dehydrogenated products, which are undesirable products, during MCH ring opening reaction by using an appropriate formulation of Pd–Rh bimetallic catalyst. In the bimetallic catalysts (results not shown), Pd contributes to limit the formation of cracking products

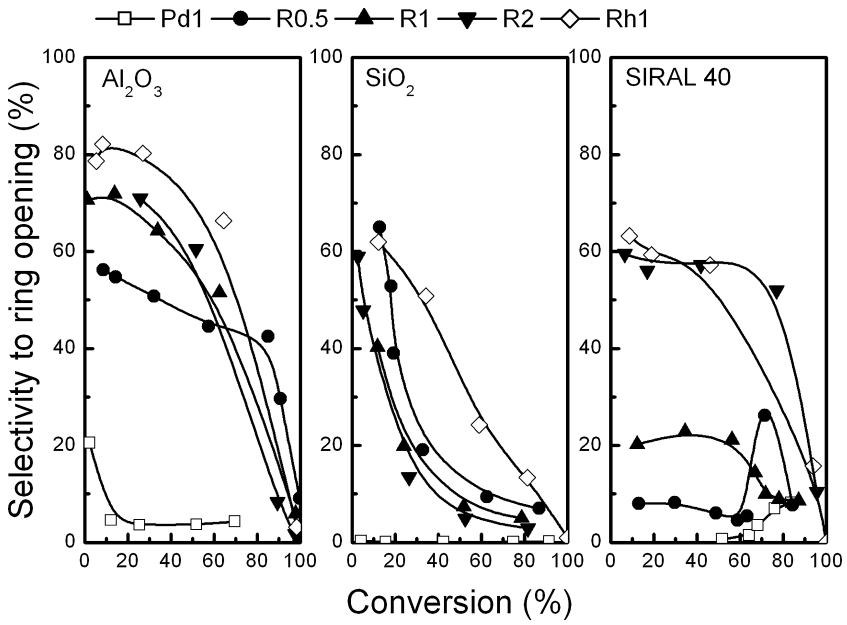

Fig. 8. Selectivity to ring opening products as a function of the MCH conversion for the three series of catalysts.

(negligible cracking reactions are observed on Pd1 samples, whatever the support) and Rh contributes to limit the dehydrogenation of MCH to toluene.

3.8. Decalin ring opening

On bifunctional catalysts the hydroconversion of decalin occurs through two parallel reactions [60,61]: ring contraction on Bronsted acid sites yielding skeletal isomers with five-membered naphthenic rings (ring contraction products) followed by hydrogenolysis of these isomers on metal sites to C_{10} one-ring naphthenes (ring opening products), as well as direct hydrogenolysis on metal sites yielding ring opening which is less favored in the case of six-membered naphthenic rings. Also a second ring opening step can occur from C_{10} one-ring naphthenes leading to open chain decane isomers, as well as cracking of RO and dehydrogenation of decalin.

The decalin reaction products were classified according to the same criterion used in a previous work [62]. The products of reaction are lumped into: cracking products (C_1–C_9 products); ring opening (RO) C_{10} products; ring contraction (RC) products; and dehydrogenated products (naphthalene and heavy dehydrogenated products). The results of the decalin reaction are presented in Fig. 11, in terms of percentages of *cis* and *trans* decalin and the selectivity to cracking, RC, RO and dehydrogenated products obtained after 6 h reaction time at 350 °C.

On acid catalysts, *trans*/*cis* decalin ratios were observed to increase in the course of the reaction, which could be due to a higher reactivity of the *cis* isomer [12,63] and also to the catalytic *cis*/*trans* isomerization reaction [64]. On Al_2O_3 and SIRAL 40 series,

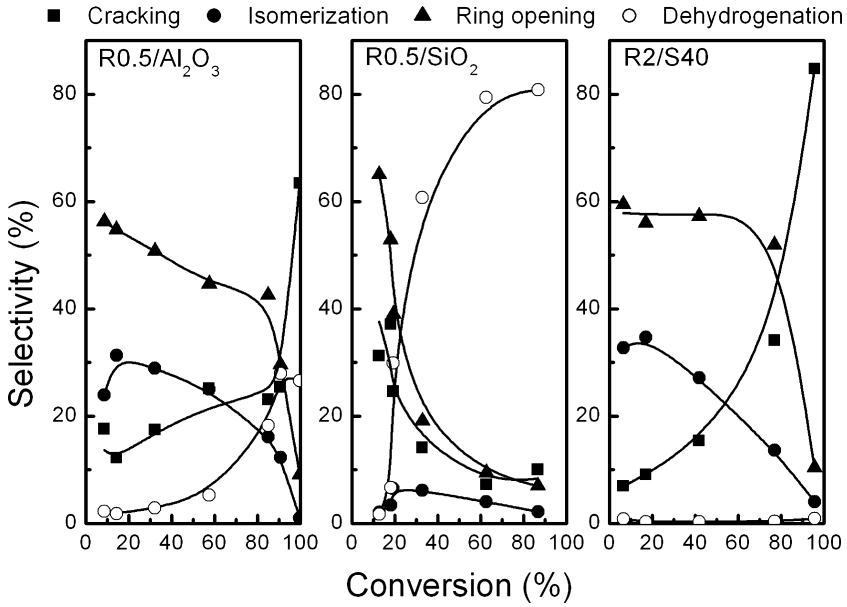

Fig. 9. Selectivity to cracking, isomerization, ring opening and dehydrogenated products as a function of the MCH conversion for the R0.5/Al_2O_3, R0.5/SiO_2 and R2/SIRAL40 catalysts.

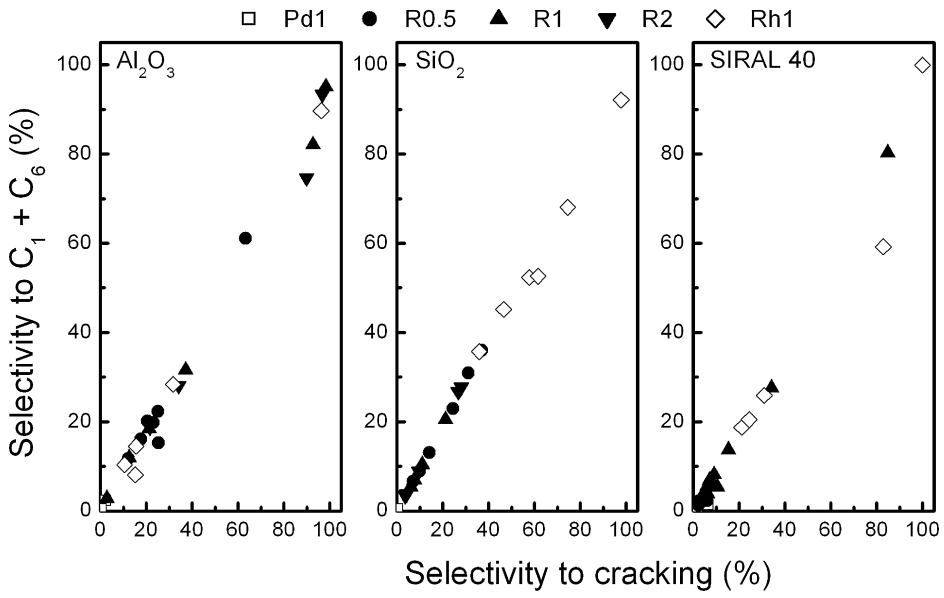

Fig. 10. C_1 and C_6 products as a function of selectivity to cracking obtained during MCH reaction for the three series of catalysts.

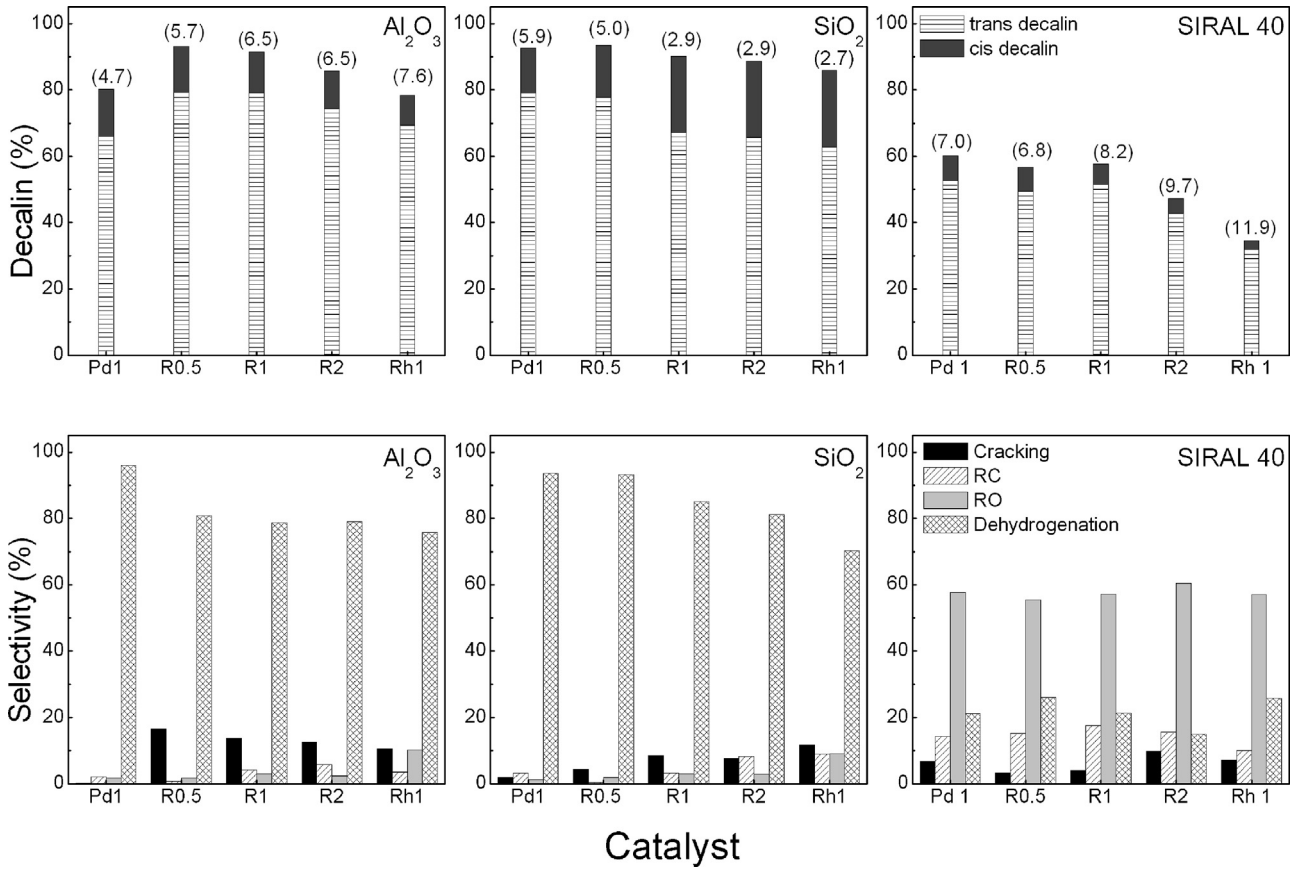

Fig. 11. *Trans* and *cis*-decalin and the selectivity to cracking, ring contraction, ring opening and dehydrogenated products obtained after 6 h reaction time. Values between brackets are *trans*/*cis*-decalin ratio.

the *trans*/*cis* ratio decalin roughly increases as a function of the conversion (initially the *trans*/*cis* ratio is of 1.63). These results are in agreement with those reported by Lai and Song [65] and Moraes et al. [66]. The Rh1 and bimetallic catalysts supported on SiO_2 show higher amounts of *cis*-decalin than their counterparts on Al_2O_3 or SIRAL 40. The lowest acidity of these samples forces the reaction to proceed on the metal function where both isomers have the same reactivity. Finally, the SIRAL 40 series have a higher *trans*/*cis* decalin ratio than the corresponding catalysts of Al_2O_3 and SiO_2 series. It is known that *cis*-decalin is more selectively converted to RO products than *trans*-decalin [12]. In general, a lower amount of *cis*-decalin obtained at the end of the reaction corresponds to

higher yields in RO products. The stereoisomerization of *cis*-decalin to *trans*-decalin occurs on the metal sites via a hydrogenation-dehydrogenation mechanism. Besides, the acid sites promote the stereoisomerization. The isomerization is an essential step in the ring opening of decalin and occurs on Brønsted acid sites. In the absence of Bronsted acid sites, no isomerization occurs nor ring opening [7,8]. This is evidenced by the results of Fig. 11, where the catalysts supported on Al_2O_3 and SiO_2 with the lowest total and Brønsted acidities show the lowest conversion, i.e., a high percentage of decalin in the final reaction medium, and a very low selectivity to RC and RO. Al_2O_3 and SiO_2 supported samples produce mainly dehydrogenated compounds (naphthalene and others). On the contrary, SIRAL 40 series, which is the most active, exhibits the best selectivity to RO products. On this support, the activity is enhanced by the increase in the Rh content, highlighting the importance of the balance between the hydrogenolytic function (Rh) and the acid sites for selective ring opening. Moreover, R2/S40 catalyst having the highest metal-metal interaction and the highest acidity of the SIRAL 40 series displays a slightly better selectivity to RO. In the Al_2O_3 and SiO_2-supported catalysts series, the increase in Rh content produces a slight increase of the conversion, which is associated with the increase in cracking products in the SiO_2 series.

The selectivity to ring contraction products is higher for the SIRAL 40 series than for the SiO_2 and Al_2O_3 ones. This trend clearly shows the importance of the acidity on the overall performance of the catalyst, the RC compounds being furthermore more easily transformed into RO products [4].

3.9. Comparison between MCH and decalin reactions

Comparison of MCH and decalin conversion is not applicable because the decalin reaction was performed in batch reactor and the MCH one in continuous flow reactor. However, selectivities values observed at the same reaction temperature could be useful to evaluate the catalysts.

As already seen, the SIRAL 40 supported catalysts notably exhibit better performances in the decalin reaction (higher conversion and higher selectivity to ring opening products) than those supported on Al_2O_3 or SiO_2 (Fig. 11). Moreover, there is no major variation in the RO selectivity between the SIRAL 40 supported catalysts. Consequently, the acidity of these catalysts plays a more important role than the metal function in decalin RO as compared to the conversion of MCH. The metal function of the catalyst plays a more relevant role in the opening of naphthenes of one ring such as MCH, compared to the one of two rings. Indeed, the rhodium content produces a marked increase in the selectivity to cracking products in the MCH reaction (Fig. 9), whereas this effect remains negligible in decalin ring opening.

In the MCH reaction, the monometallic Pd/SiO_2 catalyst produces very little amounts of RC products by isomerization, due to a low acidity. Higher amounts of isomers are obtained on Pd supported on Al_2O_3 and SIRAL 40, due to the higher acidity of these samples combined with the low hydrogenolysis activity of Pd, which limits the conversion of the formed five-membered rings. The incorporation of Rh leads to catalysts with a higher hydrogenolysis activity, and, as a consequence the RC products are transformed. Furthermore, during the decalin RO reaction, only SIRAL 40 supported catalysts produce significant amounts of RC products, highlighting that strong acid sites are required to produce ring contraction of double rings.

Finally, the results of the MCH reaction are in agreement with the parameter based on demanding/no demanding metal catalyzed reactions, while, in the decalin reaction, the acid function dominates. The higher influence of the metal function on the conversion and selectivity of MCH reaction is probably due to the lower stability of one-ring compounds compared to that of two-ring compounds. Moreover, for the decalin and MCH ring opening reactions, a first step consisting of ring contraction is necessary to facilitate the hydrogenolysis reaction.

4. Conclusions

Hydrogen chemisorption showed that the metal dispersion of the catalysts varied between 30 and 50%. Monometallic Pd/Al_2O_3 catalyst formed agglomerated nanoparticles with low metal-support interactions. Bimetallic particles were seemingly difficult to obtain on the alumina support. The same trend was observed on silica. The bimetallic catalysts supported on SIRAL 40 presented large particles of Pd and small bimetallic particles. The CP conversion/CH conversion ratio (parameter of demanding/no demanding metal catalyzed reaction) increased with the Rh content. Moreover in most cases, the CP/CH ratio was higher on the Al_2O_3 supported catalysts than in the SiO_2 and SIRAL 40 series.

The SIRAL series 40 had the highest concentration of strong acid sites, whereas the concentration of weak and moderate acid sites was higher on alumina than on silica. The following order of total and Brønsted acidities was found for the three series: SIRAL 40 » Al_2O_3 > SiO_2. For the three series, the incorporation of metals increased the acidity of the support and the strength of the acid sites decreased by increasing the Rh content.

The best support for the ring opening of MCH was Al_2O_3, whereas SIRAL 40 had the best performances for SRO of decalin, SiO_2 support being inappropriate in both reactions. The addition of Rh to Pd resulted in an increase in MCH conversion and in the formation of cracking products, while decreasing the isomerization and dehydrogenation products.

At equal values of metal dispersion and metal content, the catalysts with higher amount of total and Bronsted acid sites (i.e., supported on SIRAL 40) showed higher selectivity to RO products during SRO of decalin.

Acknowledgement

The authors gratefully acknowledge the ECOS-MINCyT program n○ A12E02 (2013-2015) which allowed the collaboration between the two research teams.

References

[1] V.P. Thakkar, S.F. Abdo, V.A. Gembicki, J.F. McGehee, In: Proc. NPRA, Annual Meeting, San-Francisco, 13-15 March 2005, UOP LLC, Des Plaines, Illinois, USA, AM-05-53.
[2] W.C. Baird, J.G. Chen, G.B. McVicker US Patent 6623626 B2, 2003 (to Exxon-Mobil).
[3] R.C. Santana, P.T. Do, M. Santikunaporn, W.E. Alvarez, J.D. Taylor, E.L. Sughrue, D.E. Resasco, Fuel 85 (2006) 643–656.
[4] G.B. McVicker, M. Daage, M.S. Touvelle, C.W. Hudson, D.P. Klein, W.C. Baird Jr., B.R. Cook, J.G. Chen, S. Hantzer, D.E.W. Vaughan, E.S. Ellis, O.C. Feeley, J. Catal. 210 (2002) 137–148.
[5] P.T.M. Do, S. Crossley, M. Santikunaporn, D.E. Resasco, Catalysis 20 (2007) 33–64.
[6] C. Marcilly, Catalyse acido-basique, in: Application au raffinage et à la pétrochimie, Editions Technip, vol, 2003, pp. 1, Chapter 4.
[7] D. Kubička, N. Kumar, P. Mäki-Arvela, M. Tiitta, V. Niemi, T. Salmi, D.Y. Murzin, J. Catal. 222 (2004) 65–79.
[8] A. Corma, V. González-Alfaro, A.V. Orchillés, J. Catal. 200 (2001) 34–44.
[9] H.S. Cerqueira, P.C. Mihindou-Koumba, P. Magnoux, M. Guisnet, Ind. Eng. Chem. Res. 40 (2001) 1032–1041.
[10] M.A. Arribas, J.J. Mahiques, A. Martínez, Stud. Surf. Sci. Catal. 135 (2001) 303.
[11] M.A. Arribas, A. Martínez, Appl. Catal. A-Gen. 230 (2002) 203–217.
[12] M. Santikunaporn, J.E. Herrera, S. Jongpatiwut, D.E. Resasco, W.E. Alvarez, J. Catal. 228 (2004) 100–113.
[13] D. Kubička, N. Kumar, P. Mäki-Arvela, M. Tiitta, V. Niemi, H. Karhu, T. Salmi, D.Y. Murzin, J. Catal. 227 (2004) 313–327.
[14] M.A. Arribas, A. Corma, M.J. Díaz-Cabañas, A. Martínez, Appl. Catal. A-Gen. 273 (2004) 277–286.
[15] H. Liu, X. Meng, D. Zhao, Y. Li, Chem. Eng. J. 140 (2008) 424–431.

[16] G. Onyestyak, G. Pál-Borbély, H. Beyer, Appl. Catal. A-Gen. 229 (2002) 65–67.
[17] S. Lecarpentier, J. Van Gestel, K. Thomas, J.-P. Gilson, M. Houalla, J. Catal. 254 (2008) 49–63.
[18] W. Baird, D. Klein, J. Chen, G. McVicker, US Patent 6683020 B2, 2004 (to Exxon-Mobil).
[19] S. Lecarpentier, J. Van Gestel, J.-P. Dath, C. Collet, J.-P. Gilson, WO Patent Application 2007006924 A8, 2007 (to Total-France).
[20] L.M. Kustov, T.V. Vasina, O.V. Hasloboishchikova, E.G. Khelkovskaya, P. Zeuthen, Stud. Surf. Sci. Catal. 130 (2000) 227–232.
[21] D. Teschner, L. Pirault-Roy, D. Naud, M. Guerin, Z. Paál, Appl. Catal. A-Gen. 252 (2003) 421–426.
[22] F.G. Gault, Adv. Catal. 30 (1981) 1–9.
[23] Z. Paál, P. Tétényi, Nature 267 (1977) 234–236.
[24] J.L. Carter, J.A. Cusumano, J.H. Sinfelt, J. Catal. 20 (1971) 223–229.
[25] C.G. Walter, B. Coq, F. Figueras, M. Boulet, Appl. Catal. A-Gen. 133 (1995) 95–102.
[26] M. Taillades-Jacquin, D.J. Jones, J. Rozière, R. Moreno-Tost, A. Jiménez-López, S. Albertazzi, A. Vaccari, L. Storaro, M. Lenarda, J.M. Trejo-Menayo, Appl. Catal. A-Gen. 340 (2008) 257–264.
[27] G. Crépeau, V. Montouillou, A. Vimont, L. Marey, T. Cséri, F. Maugé, J. Phys. Chem. B 110 (2006) 15172–15185.
[28] E.J.M. Hensen, D.G. Poduval, D.A.J.M. Ligthart, J.A.R. van Veen, M.S. Rigutto, J. Phys. Chem. C 114 (2010) 8363–8374.
[29] S.A. D'Ippolito, C. Especel, L. Vivier, F. Epron, C.L. Pieck, Appl. Catal. A-Gen. 469 (2014) 532–540.
[30] S.A. D'Ippolito, C. Especel, L. Vivier, F. Epron, C.L. Pieck, Appl. Catal. A-Gen. 469 (2014) 541–549.
[31] L.S. Carvalho, K.C.S. Conceição, V.A. Mazzieri, P. Reyes, C.L. Pieck, M.C. Rangel, Appl. Catal. A-Gen. 419-420 (2012) 156–163.
[32] P. Samoila, F. Epron, P. Marecot, C. Especel, Appl. Catal. A-Gen. 462-463 (2013) 207–219.
[33] L.S. Carvalho, C.L. Pieck, M.C. Rangel, N.S. Fígoli, C.R. Vera, J.M. Parera, Appl. Catal. A-Gen. 269 (2004) 105–116.
[34] J.I. Villegas, D. Kubička, H. Karhu, H. Österholm, N. Kumar, T. Salmi, D.Y. Murzin, J. Mol. Catal. A: Chem. 264 (2007) 192–201.
[35] D. Kubička, N. Kumar, T. Venäläinen, H. Karhu, I. Kubičková, H. Österholm, D.Y. Murzin, J. Phys. Chem. B 110 (2006) 4937–4946.
[36] L.M. Kustov, T.V. Vasina, A.V. Ivanov, O.V. Masloboishchikova, E.V. Khelkovskaya-Sergeeva, P. Zeuthen, Stud. Surf. Sci. Catal. 101 (1996) 821–830.
[37] A.K. Aboul-Gheit, S.M. Abodoul-Fotouh, N.A.K. Abodoul-Gheit, Appl. Catal. A-Gen. 292 (2005) 144–153.
[38] A.K. Aboul-Gheit, S.M. Abodoul-Fotouh, S.M. Abdel-Hamid, N.A.K. Abodoul-Gheit, J. Mol. Catal. A: Chem. 245 (2006) 167–177.
[39] J. Valyon, J. Engelhardt, F. Lónyi, D. Kalló, Á. Gömöry, Appl. Catal. A-Gen. 229 (2002) 135–146.
[40] V. Nieminen, M. Kangas, T. Salmi, D.Y. Murzin, Ind. Eng. Chem. Res. 44 (2005) 471–484.
[41] A.Y. Stakheev, L.M. Kustov, Appl. Catal. A-Gen. 188 (1999) 3–35.
[42] C. Kemball, H.F. Leach, B. Skundric, K.C. Taylor, J. Catal. 27 (1972) 416–423.
[43] C.S. John, C. Kemball, R.A. Rajadhayarsha, J. Catal. 57 (1979) 264–271.
[44] E.A. Irvine, C.S. John, C. Kemball, A.J. Pearman, M.A. Day, R.J. Sampson, J. Catal. 61 (1980) 326–335.
[45] H. Lieske, J. Völter, J. Phys. Chem. 89 (1985) 1841–1842.
[46] A. Aylor, L. Lobree, J. Reimer, A.T. Bell, J. Catal. 172 (1997) 453–462.
[47] A.M. Venezia, L. Liotta, G. Deganello, P. Terreros, M. Pena, J.L.G. Fierro, Langmuir 15 (1999) 1176–1181.
[48] W. Juszczyk, Z. Karpinski, I. Ratajczykowa, Z. Stanasiuk, J. Zielinski, L.L. Shen, W.M.H. Sachtler, J. Catal. 120 (1989) 68–77.
[49] G.C. Cabilla, A.L. Bonivardi, M.A. Baltanás, Catal. Lett. 55 (1998) 147–156.
[50] A.C. Yang, C.W. Garland, J. Phys. Chem. 61 (1957) 1504–1512.
[51] A.K. Smith, F. Hugues, A. Theolier, J.M. Basset, R. Ugo, G.M. Zanderighi, J.L. Bilhou, V. Bilhou-Bougnal, W.F. Graydon, Inorg. Chem. 18 (1979) 3104–3112.
[52] S. Trautmann, M. Baerns, J. Catal. 150 (1994) 335–344.
[53] P.B. Rasband, W.C. Hecker, J. Catal. 139 (1993) 551–560.
[54] O. Dulaurent, K. Chandes, C. Bouly, D. Bianchi, J. Catal. 192 (2000) 262–272.
[55] H.F.J. Van't Blik, J.B.A.D. Van Zon, T. Hulzinga, J.C. Vis, J.C. Koningsberger, R. Prins, J. Phys. Chem. 87 (1983) 2264–2267.
[56] M. Boudart, Adv. Catal. Rel. Sub. 20 (1969) 153–166.
[57] J. Weitkamp, A. Raichle, Y. Traa, Appl. Catal. A-Gen. 222 (2001) 277–297.
[58] A. Raichle, Y. Traa, J. Weitkamp, Appl. Catal. B-Environ. 41 (2003) 193–205.
[59] P. Samoila, M. Boutzeloit, I. Salem, D. Uzio, G. Mabilon, F. Epron, P. Marécot, C. Especel, Appl. Catal. A-Gen. 415-416 (2012) 80–88.
[60] M. Al-Sabawi, H. de Lasa, Chem. Eng. Sci. 65 (2010) 626–644.
[61] S. Rabl, A. Haas, D. Santi, C.M. Flego, M. Ferrari, V. Calemma, G. Bellussi, J. Weitkamp, Microporous Mesoporous Mater. 146 (2011) 190–200.
[62] S.A. D'Ippolito, L.B. Gutierrez, C.L. Pieck, Appl. Catal. A-Gen. 445-446 (2012) 195–203.
[63] E.F. Sousa-Aguiar, C.J.A. Mota, M.L. Valle Murta, M. Pinhel da Silva, D. Forte da Silva, J. Mol. Catal. A: Chem. 104 (1996) 267–271.
[64] R.C. Schucker, J. Chem. Eng. Data 26 (1981) 239–241.
[65] W.C. Lai, C. Song, Catal. Today 31 (1996) 171–181.
[66] R. Moraes, K. Thomas, S. Thomas, S. Van Donk, G. Grasso, J.-P. Gilson, M. Houalla, J. Catal. 286 (2012) 62–77.